

Lattice Electrodynamics in Primal and Dual Spaces

Bo He* and F. L. Teixeira†

*ElectroScience Laboratory and Department of Electrical and Computer Engineering,
The Ohio State University, 1320 Kinnear Road, Columbus, OH 43212, USA*

(Dated: April 14, 2019)

Abstract

Based on a geometric discretization scheme for Maxwell equations, we unveil a mathematical transformation between the electric field intensity E and the magnetic field intensity H , denoted as Galerkin duality. Using Galerkin duality and discrete Hodge operators, we construct two system matrices, $[X_E]$ (primal formulation) and $[X_H]$ (dual formulation) respectively, that discretize the second-order vector wave equations. We show that the primal formulation recovers the conventional (edge-element) finite element method (FEM) and suggests a geometric foundation for it. On the other hand, the dual formulation suggests a new (dual) type of FEM. Although both formulations give identical dynamical physical solutions, the dimensions of the null spaces are different.

PACS numbers: 02.70.Dh; 03.50.De; 02.60.-x; 41.20.-q

*Electronic address: he.87@osu.edu

†Electronic address: teixeira.5@osu.edu

I. INTRODUCTION

The finite element method (FEM) originally developed for structure design and analysis is usually based on nodal elements [1]. Simply applying nodal elements to Maxwell equations causes problems such as spurious modes [2]. The use of edge elements is the most reasonable way [3] to remove the spurious modes because the electric field intensity E is a differential 1-form associated with the edges [19]

The basic strategy of traditional FEM (Galerkin's method) is to seek the solution by weighting the residual of the second-order wave equations. Here, we adopt a different route. Based on a general discretization scheme for Maxwell equations on irregular lattices, we construct two system matrices in terms of the electric field intensity E (denoted as primal formulation) and the magnetic field intensity H (denoted as dual formulation), respectively. The primal formulation recovers the FEM based on edge elements, and suggests a geometric foundation for it. On the other hand, the dual formulation suggests a new (dual) type of FEM. Although both formulations give identical physical solutions, the dimensions of the null (kernel) spaces are different. The connection between the primal formulation and dual formulation is established via a transformation, denoted here as *Galerkin duality* (not to be confused with conventional electromagnetic duality [5][6])

II. DISCRETE MAXWELL EQUATIONS

Maxwell equations in source-free, three-dimensional (3D) space (in the Fourier domain) are written in terms of differential forms [7][8] as

$$dE = i\omega B, \quad dB = 0, \quad dH = -i\omega D, \quad dD = 0 \quad (1)$$

where E and H are electric and magnetic field intensity 1-forms, D and B are electric and magnetic flux 2-forms, and d is the (metric-free) exterior derivative operator. Constitutive equations, which include all metric information, are written in terms of Hodge (star) operators (that fix an isomorphism between p -forms and $(3 - p)$ -forms) [7]

$$D = \star_{\epsilon} E, \quad B = \star_{\mu} H \quad (2)$$

By applying basic tools of algebraic topology and a discrete analog of differential forms, discrete electromagnetic theory can be constructed from first principles on a general (irreg-

ular) primal/dual lattice (cell-complex) [7]. The discrete Maxwell equations read as [9]

$$[d_{curl}] \mathbb{E} = i\omega \mathbb{B}, [d_{div}] \mathbb{B} = 0, [d_{curl}^*] \mathbb{H} = -i\omega \mathbb{D}, [d_{div}^*] \mathbb{D} = 0 \quad (3)$$

where $\mathbb{E}, \mathbb{B}, \mathbb{H}, \mathbb{D}$ are arrays of degrees of freedom (*DoFs*) and $[d_{curl}], [d_{div}], [d_{curl}^*], [d_{div}^*]$ are *incidence matrices* that encode the discrete exterior derivatives (discrete counterparts to the curl and divergence operators, distilled from their metric structure) on the primal and dual lattice, respectively. Due to the absence of metric structure, entries of the incidence matrices assume only $\{-1, 0, 1\}$ values [7].

The discrete Hodge operators can be, in general, written as follows

$$\mathbb{D} = [\star_\epsilon] \mathbb{E}, \mathbb{B} = [\star_\mu] \mathbb{H} \quad (4)$$

One approach to construct the Hodge matrices $[\star_\epsilon]$ and $[\star_\mu]$ will be discussed in next Section. In addition to being non-singular, the Hodge matrices should be symmetric (in reciprocal media) and positive definite (in passive media) to obtain stable discretizations for time-domain simulations [7].

III. DISCRETE HODGE OPERATORS

Let Ω be a n -dimensional differentiable manifold and $F^p(\Omega)$ the space of forms of p -degree defined on it. If Ω is endowed with a metric, then the Hodge operator $\star : \eta \rightarrow \xi = \star\eta$ [10][11] is defined as a map of $\eta \in F^p(\Omega)$ to $\xi \in F^{n-p}(\Omega)$ such that for any $\psi \in F^p(\Omega)$

$$\int_{\Omega} \psi \wedge \xi = \int_{\Omega} \psi \wedge \star\eta \quad (5)$$

The Hodge operator defines (through a metric) an infinite dimensional inner product, denoted as (ψ, η)

$$(\psi, \eta) = \int_{\Omega} \psi \wedge \star\eta \quad (6)$$

For some form ψ we can also define the Hodge square of ψ by

$$(\psi, \psi) = \int_{\Omega} \psi \wedge \star\psi \quad (7)$$

which is positive when the metric is positive definite. By applying (7) to electric field and magnetic field, one can obtain constitutive relations in terms of Hodge operators in 3D

Euclidean space R^3 as

$$(E, E) = \int_{R^3} E \wedge D = \int_{R^3} E \wedge \star_\epsilon E \quad (8)$$

$$(B, B) = \int_{R^3} B \wedge H = \int_{R^3} B \wedge \star_{\mu^{-1}} B \quad (9)$$

Whitney forms [12] are the basic interpolants for discrete differential forms of various degrees defined over tetrahedra. Whitney forms can be expressed in term of the barycentric coordinates associated with each tetrahedron node $(\zeta_i, \zeta_j, \zeta_k, \zeta_r)$ as [13]

$$w_i^0 = \zeta_i \quad (10)$$

$$w_{i,j}^1 = \zeta_i d\zeta_j - \zeta_j d\zeta_i \quad (11)$$

$$w_{i,j,k}^2 = 2 (\zeta_i d\zeta_j \wedge d\zeta_k + \zeta_j d\zeta_k \wedge d\zeta_i + \zeta_k d\zeta_i \wedge d\zeta_j) \quad (12)$$

$$w_{i,j,k,r}^3 = 6 \begin{pmatrix} \zeta_i d\zeta_j \wedge d\zeta_k \wedge d\zeta_r - \zeta_r d\zeta_i \wedge d\zeta_j \wedge d\zeta_k \\ + \zeta_k d\zeta_r \wedge d\zeta_i \wedge d\zeta_j - \zeta_j d\zeta_k \wedge d\zeta_r \wedge d\zeta_i \end{pmatrix} \quad (13)$$

(See the appendix for the basis functions over cubes). Accordingly, we use Whitney 1-forms as the interpolants for electric field intensity 1-form E , and Whitney 2-forms as interpolants for the magnetic flux 2-form B

$$E = \sum e_{i,j} w_{i,j}^1, \quad B = \sum b_{i,j,k} w_{i,j,k}^2 \quad (14)$$

Note that the above expansions guarantee tangential continuity of E and normal continuity of B simultaneously.

Using these basis functions and the Euclidean metric, matrix representations for the Hodge operators \star_ϵ and $\star_{\mu^{-1}}$ can be constructed by combining Eq. (8), Eq. (9) and Eq. (14)

$$\begin{aligned} [\star_\epsilon]_{\{(i,j),(\tilde{i},\tilde{j})\}} &= \int_{R^3} w_{i,j}^1 \wedge \star_\epsilon w_{\tilde{i},\tilde{j}}^1 dV = (w_{i,j}^1, w_{\tilde{i},\tilde{j}}^1) \\ [\star_{\mu^{-1}}]_{\{(i,j,k),(\tilde{i},\tilde{j},\tilde{k})\}} &= \int_{R^3} w_{i,j,k}^2 \wedge \star_{\mu^{-1}} w_{\tilde{i},\tilde{j},\tilde{k}}^2 dV = (w_{i,j,k}^2, w_{\tilde{i},\tilde{j},\tilde{k}}^2) \end{aligned} \quad (15)$$

We denoted these matrices as Galerkin's discrete Hodges, or simply Galerkin's Hodges.

IV. PRIMAL AND DUAL DISCRETE WAVE EQUATIONS

A. Discrete wave equations

From Eqs.(3), (4) and (15), two discrete, second-order vector wave equations can be obtained

$$[d_{curl}^*][\star_{\mu^{-1}}][d_{curl}]\mathbb{E} = \omega^2[\star_{\epsilon}]\mathbb{E} \quad (16)$$

$$[d_{curl}][\star_{\epsilon}]^{-1}[d_{curl}^*]\mathbb{H} = \omega^2[\star_{\mu^{-1}}]^{-1}\mathbb{H} \quad (17)$$

corresponding to a primal and dual formulation, respectively. These are the discrete analogs of the curl curl equations

$$\vec{\nabla} \frac{1}{\mu} \times \vec{\nabla} \times \vec{E} = \omega^2 \epsilon \vec{E} \quad (18)$$

$$\vec{\nabla} \frac{1}{\epsilon} \times \vec{\nabla} \times \vec{H} = \omega^2 \mu \vec{H} \quad (19)$$

It can be shown that $[d_{curl}^*][\star_{\mu^{-1}}][d_{curl}]$ is identical to the conventional stiffness matrix $[S]$ (see Appendix), arising in FEM using edge elements

$$[S]_{\{(i,j),(\tilde{i},\tilde{j})\}} = \int \frac{1}{\mu} \left(\vec{\nabla} \times \vec{W}_{i,j}^1 \right) \cdot \left(\vec{\nabla} \times \vec{W}_{\tilde{i},\tilde{j}}^1 \right) dV \quad (20)$$

Hence, the primal formulation recovers the conventional edge-element FEM and suggests a geometric foundation for it. For the dual formulation, we can introduce dual stiffness $[S^\dagger]$ and mass $[M^\dagger]$ matrices

$$[S^\dagger] = [d_{curl}][\star_{\epsilon}]^{-1}[d_{curl}^*] \quad (21)$$

$$[M^\dagger] = [\star_{\mu^{-1}}]^{-1} \quad (22)$$

This dual formulation has no direct counterpart in traditional FEM. As discussed next, these two formulations lead to the same dynamic solutions, but have very different mathematical properties.

B. Galerkin duality

Galerkin duality is a mathematical transformation between the above primal and dual formulations. Note that Galerkin duality is distinct from usual electromagnetic duality [5][6], as illustrated in Table I.

TABLE I: Galerkin duality vs. Electromagnetic duality.

$\vec{E} \rightarrow \vec{H}, \vec{H} \rightarrow -\vec{E}$	$\vec{E} \rightarrow \vec{H}, \vec{H} \rightarrow -\vec{E}$
PEC→PEC	PEC→PMC
Dirichlet BC→Neumann BC	Dirichlet BC→Dirichlet BC
Neumann BC→Dirichlet BC	Neumann BC→Neumann BC

Based on Galerkin duality and the discrete Hodge operators introduced before, we can construct two different system matrices for a given problem

$$[X_E] = [\star_\epsilon]^{-1} [d_{curl}^*] [\star_{\mu^{-1}}] [d_{curl}] \quad (23)$$

$$[X_H] = [\star_{\mu^{-1}}] [d_{curl}] [\star_\epsilon]^{-1} [d_{curl}^*] \quad (24)$$

Both $[X_E]$ and $[X_H]$ encode all discrete *dynamic* information, and hence produce identical dynamic solutions. However, their null spaces (associated with zero modes) are very different. In other words, for a discretization of the same physical system, the dimensions of the (discrete) zero eigenspaces are different under Galerkin duality. This can be explained by algebraic properties of discrete Hodge decomposition, and verified by numerical simulations, as discussed in Section V.

C. A approach to handle Neumann boundary condition

Since Dirichlet boundary condition and Neumann boundary condition are Galerkin dual to each other for some underlying differential equations, we propose an approach to handle Neumann boundary condition. Consider a differential equation

$$\Theta\phi = 0 \quad (25)$$

where Θ is a differential operator and ϕ is the unknown physical quantity, with Neumann boundary condition. By Galerkin duality, this problem is equivalent to solving

$$\Theta^\dagger\phi^\dagger = 0 \quad (26)$$

with Dirichlet boundary condition. Here Θ^\dagger is the Galerkin dual to Θ , and ϕ^\dagger is the Galerkin dual to ϕ . ϕ^\dagger can be expanded by basis functions W_i^\dagger

$$\phi^\dagger = \sum \phi_i^\dagger W_i^\dagger \quad (27)$$

For some problems, the benefit of the formulation (26) is that the basis functions W_i^\dagger can be easier to build so that Dirichlet boundary condition is enforced directly. Moreover, the number of *DoFs* of discretization ϕ^\dagger may be considerably smaller than that of ϕ .

V. EXAMPLES

To demonstrate the Galerkin duality, we provide some numerical simulations for 2D cavity problems in the (x, y) plane. Both TE and TM cases are simulated. The finite element meshes for these examples were generated by using Triangle, a freely available 2D mesh generator [14]. The angular frequencies of the resonant modes are obtained by solving the eigenvalue equation (16) (primal formulation) or the eigenvalue equation (17) (dual formulation). For simplicity, we set $\epsilon = \mu = 1$.

A. Whitney forms in 2D

The vector calculus proxies of Whitney forms in 2D can be written in term of barycentric coordinates $(\zeta_i, \zeta_j, \zeta_k)$ as

$$W_i^0 = \zeta_i \tag{28}$$

$$\vec{W}_{i,j}^1 = \zeta_i \nabla \zeta_j - \zeta_j \nabla \zeta_i \tag{29}$$

$$W_{i,j,k}^2 = 2(\zeta_i \nabla \zeta_j \times \nabla \zeta_k + \zeta_j \nabla \zeta_k \times \nabla \zeta_i + \zeta_k \nabla \zeta_i \times \nabla \zeta_j) \tag{30}$$

In the above, W_i^0 and $W_{i,j,k}^2$ are scalars and $\vec{W}_{i,j}^1$ is a vector.

1. TE case

For the TE case, we use the Whitney 1-forms as the interpolants for the electric field intensity \vec{E} and Whitney 2-forms as the interpolants for the magnetic flux B_z

$$\vec{E} = \sum e_{i,j} \vec{W}_{i,j}^1, \quad B_z = \sum b_{i,j,k} W_{i,j,k}^2 \tag{31}$$

TABLE II: TE vs. TM.

	E	B
Degree of differential-form (TE)	1	2
Degree of differential-form (TM)	0	1
Element (TE)	edge	face
Element (TM)	node	edge

Vector calculus proxies of the Galerkin's Hodges become

$$\begin{aligned}
[\star_\epsilon]_{\{(i,j),(\tilde{i},\tilde{j})\}} &= \int \epsilon \vec{W}_{i,j}^1 \cdot \vec{W}_{\tilde{i},\tilde{j}}^1 dS \\
[\star_{\mu^{-1}}]_{\{(i,j,k),(\tilde{i},\tilde{j},\tilde{k})\}} &= \int \frac{1}{\mu} W_{i,j,k}^2 \cdot W_{\tilde{i},\tilde{j},\tilde{k}}^2 dS
\end{aligned} \tag{32}$$

2. TM case

For the TM case, we use the Whitney 0-forms as the interpolants for the electric field intensity E_z and Whitney 1-forms as the interpolants for the magnetic flux \vec{B}

$$E_z = \sum e_i W_i^0, \quad \vec{B} = \sum b_{i,j} \vec{W}_{i,j}^1 \tag{33}$$

Vector calculus proxies of the Galerkin's Hodges become

$$\begin{aligned}
[\star_\epsilon]_{\{i,\tilde{i}\}} &= \int \epsilon W_i^0 \cdot W_{\tilde{i}}^0 dS \\
[\star_{\mu^{-1}}]_{\{(i,j),(\tilde{i},\tilde{j})\}} &= \int \frac{1}{\mu} \vec{W}_{i,j}^1 \cdot \vec{W}_{\tilde{i},\tilde{j}}^1 dS
\end{aligned} \tag{34}$$

The comparison between TE and TM case is illustrated in Table II

B. Circular cavity

Table III and Table IV present the results for TE modes and TM modes of a circular cavity with radius $a = 1$. The analytical solutions of TE modes are the zeros of Bessel function derivative $J'_m(x)$; The analytical solutions of TM modes are the zeros of Bessel function $J_m(x)$. Note that TE_{mn} and TM_{mn} have a twofold degeneracy analytically if $m \neq 0$. However, the numerical solutions break the degeneracy. From the Table III (2D TE modes), we find that the number of zero modes of primal formulation is equal to the

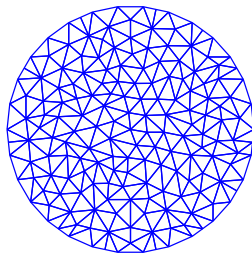


FIG. 1: The mesh has 178 vertices (136 internal vertices), 447 internal edges and 312 triangles.

TABLE III: TE modes (the angular frequencies of the 5 lowest nonzero modes) of a circular cavity.

Mode TE_{mn}	Primal	Dual	Analytical	Error(%)
TE_{11}	1.8493	1.8493	1.8412	0.4416
TE_{11}	1.8494	1.8494	1.8412	0.4483
TE_{21}	3.0707	3.0707	3.0542	0.5381
TE_{21}	3.0708	3.0708	3.0542	0.5412
TE_{01}	3.8421	3.8421	3.8317	0.2705
# zero modes	136	1		
# nonzero modes	311	311		

number of internal nodes, while the number of zero modes of dual formulation is 1. On the other hand, from the Table IV (2D TM modes), we find that the number of zero modes of primal formulation is 0, while the number of zero modes of dual formulation is $N_F - 1$. From the last rows of Table III and Table IV, we conclude that both formulations give the same number of nonzero modes. These numerical facts, summarized in Table V, will be explained by applying a discrete Hodge decomposition in next subsection.

C. Discrete Hodge decomposition

In a contractible domain Ω , the Hodge decomposition for a p -form in $F^p(\Omega)$ can be written as [15]

$$F^p(\Omega) = dF^{p-1}(\Omega) \oplus \delta F^{p+1}(\Omega) \quad (35)$$

TABLE IV: TM modes (the angular frequencies of the 5 lowest nonzero modes) of a circular cavity.

Mode TM_{mn}	Primal	Dual	Analytical	Error(%)
TM_{01}	2.4206	2.4206	2.4048	0.6569
TM_{11}	3.8883	3.8883	3.8317	1.4758
TM_{11}	3.8901	3.8901	3.8317	1.5234
TM_{21}	5.2669	5.2699	5.1356	2.5563
TM_{21}	5.2694	5.2694	5.1356	2.6050
# zero modes	0	311		
# nonzero modes	136	136		

TABLE V: Numerical results of number of modes of TE and TM.

	Primal formulation	Dual formulation
# zero modes (TE)	N_V^{in}	1
# zero modes (TM)	0	$N_F - 1$
# nonzero modes (TE)	$N_E^{in} - N_V^{in}$	$N_F - 1$
# nonzero modes (TM)	N_V^{in}	$N_E^{in} - (N_F - 1)$

where δ is the codifferential operator (Hilbert adjoint of d). An arbitrary contractible 2D domain Ω can be discretized by a general grid made up of a network of polygons. We will briefly discuss next the connection between the discrete Hodge decomposition above and the Euler's formula for a network of polygons (for a more details, see reference [9]).

1. 2D TE case

For 2D TE case, applying (35) to the electric field intensity E (1-form), we obtain

$$E^1 = d\phi^0 + \delta A^2 \quad (36)$$

where ϕ^0 is a 0-form and A^2 is a 2-form. In Eq. (36) $d\phi^0$ represents the static field and δA^2 represents the dynamic field. We can trace the following correspondence between Euler's

formula for a network of polygons and the Hodge decomposition [9]

$$\begin{aligned}
 N_E^{in} - N_V^{in} &= N_F - 1 & (37) \\
 \updownarrow \quad \updownarrow & \quad \quad \quad \updownarrow \\
 E^1 - d\phi^0 &= \delta A^2
 \end{aligned}$$

where N_V^{in} is the number of internal vertices, N_E^{in} the number of internal edges and N_F the number of faces of a mesh.

2. 2D TM case

For 2D TM case, applying (35) to the electric field intensity E (0-form), we obtain

$$E^0 = \delta A^1 \quad (38)$$

where A^1 is a 1-form. We can trace the following correspondence between Euler's formula for a network of polygons and the Hodge decomposition

$$\begin{aligned}
 N_V^{in} - 0 &= [N_E^{in} - (N_F - 1)] & (39) \\
 \updownarrow & \quad \quad \quad \updownarrow \\
 E^0 &= \delta A^1
 \end{aligned}$$

3. Zero modes and nonzero modes

Eq. (37) or Eq. (39) can be summarized as

$$L_1 - L_2 = R_1 - R_2 \quad (40)$$

For TE case, we identify

$$L_1 = N_E^{in}, L_2 = N_V^{in}, R_1 = N_F, R_2 = 1 \quad (41)$$

and for TM case, we identify

$$L_1 = N_V^{in}, L_2 = 0, R_1 = N_E^{in}, R_2 = (N_F - 1) \quad (42)$$

The l.h.s. of Eq. (40) corresponds to the range space of $[X_E]$ while the r.h.s. corresponds to the range space of $[X_H]$. Furthermore, The L_2 corresponds to the null space of $[X_E]$ while R_2 corresponds to the null space of $[X_H]$. These results are summarized in Table VI.

TABLE VI: Null spaces and range space of $[X_E]$ and $[X_H]$

	$[X_E]$	$[X_H]$
Dim(Null space) (TE)	N_V^{in}	1
Dim(Null space) (TM)	0	$N_F - 1$
Dim(Range space) (TE)	$N_E^{in} - N_V^{in}$	$N_F - 1$
Dim(Range space)(TM)	N_V^{in}	$N_E^{in} - (N_F - 1)$

Table VI exactly matches Table V from numerical results. The *DoFs* of system matrices $[X_E]$ and $[X_H]$ equal the total number of modes of primal formulation and dual formulation, respectively. Furthermore, the *DoFs* in the null space of $[X_E]$ and $[X_H]$ equal the number of zero modes of primal formulation and dual formulation, respectively; Finally the *DoFs* in the range space of $[X_E]$ and $[X_H]$ equal the number of nonzero (dynamic) modes of primal formulation and dual formulation, respectively. Note that in the case of 2D TE modes (the electric field intensity E is a 1-form interpolated by edge elements), it is a well known fact that the dimension of the null space (# zero modes) of $[X_E]$ is equal to the number of internal nodes [9][16][17].

From Eq. (40) (Euler's formula for a network of polygons) it can be concluded that the dimension of range space of $[X_E]$ equals the dimension of range space of $[X_H]$. In fact, this is a fundamental property of discrete Maxwell equations [9].

D. Polygonal cavity

A 2D cavity of arbitrary shape can be approximated by a polygon as the boundary [9]. Table VII and Table VIII present the results for TE modes and TM modes of a polygonal cavity (Fig. 2). The results support the above conclusions summarized by Table V and Table VI. Moreover, both systems matrices $[X_E]$ and $[X_H]$ are finite approximation of the corresponding infinite system. If we use same mesh and same basis functions, that is, same basic matrices $[d_{curl}]$, $[d_{curl}^*]$, $[\star_{\mu^{-1}}]$ and $[\star_{\epsilon}]$, the dynamic physical structure encoded by system matrices $[X_E]$ and $[X_H]$ will be same. Furthermore, if we use same linear solver, the solutions of both formulations will give the *identical* nonzero modes (dynamic solutions) up to round off errors (see Table VII and VIII).

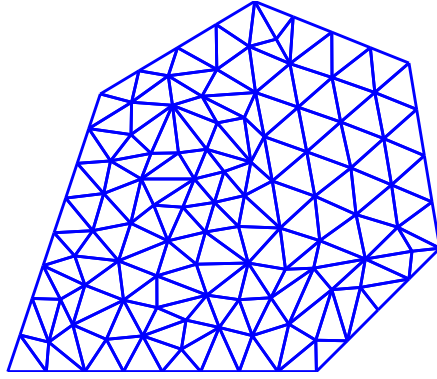


FIG. 2: The coordinates of the vertices of the polygon are $(0,0)$, $(1,0)$, $(1.4,0.4)$, $(1.3,1.0)$, $(0.8,1.2)$, $(0.3,0.9)$. The mesh has 105 vertices (73 internal vertices), 248 internal edges and 176 triangles.

TABLE VII: TE modes (the angular frequencies of the 5 lowest nonzero modes) of a polygonal cavity.

Mode No. (TE)	Primal formulations	Dual formulation
1	2.57359064243139	2.57359064243165
2	3.28134124800976	3.28134124800987
3	4.32578591632893	4.32578591632896
4	5.17188723866480	5.17188723866481
5	5.94586993156365	5.94586993156362
# zero modes	73	1
# nonzero modes	175	175

VI. CONCLUDING REMARKS

Based on Galerkin duality and discrete Hodge operators, we construct two system matrices, $[X_E]$ (primal formulation) and $[X_H]$ (dual formulation) that discretize the wave equations. It can be shown that the primal formulation recovers the conventional (edge-element) FEM and suggests a geometric foundation for it. On the other hand, the dual formulation suggests a new (dual) type of FEM. Although both formulations give identical physical solutions, the null spaces are different. The connection between the $DoFs$ can be associated

TABLE VIII: TM modes (the angular frequencies of the 5 lowest nonzero modes) of a polygonal cavity.

Mode No.(TM)	primal formulations	dual formulation
1	4.06172573841605	4.06172573841600
2	6.20284873300873	6.20284873300876
3	6.85765079948016	6.85765079948015
4	8.31632816148913	8.31632816148915
5	9.05550834626485	9.05550834626483
# zero modes	0	175
# nonzero modes	73	73

with Euler's formula for a network of polygons for 2D case (or polyhedra for 3D case).

-
- [1] O. C. Zienkiewicz and R. L. Taylor, *The finite Element Method* (4th edition). Vol. 1: *Basic Formulation and Linear Problems*. New York: McGraw-Hill, 1989
- [2] D. Sun, et al., "Spurious modes in finite element methods," *IEEE Trans. on Antennas and Propagat.* **37**, 12-24 (1995).
- [3] A. Bossavit, "Solving Maxwell Equations in a Closed Cavity, And the Question of 'spurious modes,'" *IEEE Tran. On Magn.*, Vol. **26**, 702-705 (1990).
- [4] Z. Ren and N. Ida, "High order differential form-based elements for the computation of electromagnetic field," *IEEE Tran. on Magn.*, **36**, 1472 (2000).
- [5] C. Balanis, *Advanced Engineering Electromagnetics*, John Wiley & Sons, New York, (1989).
- [6] W. C. Chew, *Waves and Fields in Inhomogeneous Media*, IEEE Press, Piscataway NJ (1995).
- [7] F. L. Teixeira and W. C. Chew, "Lattice electromagnetic theory from a topological viewpoint," *J. Math. Phys.* **40**, 169-187 (1999).
- [8] G. A. Deschamps, "Electromagnetics and differential forms," *Proc. IEEE* **69**, 676-696 (1981).
- [9] B. He and F. L. Teixeira, "On the degree of freedom of lattice electrodynamics", *Phys. Lett. A* **336**, 1-7 (2005).
- [10] H. Flanders, "Differential forms with applications to the physical sciences," (Dover, New

- York, 1989).
- [11] T. J. Honan, "The geometry of lattice field theory," Ph.D. thesis, University of Maryland, (1986).
 - [12] H. Whitney, "Geometric integration theory", Princeton University Press, (1957).
 - [13] A. Bossavit, "Whitney forms: a class of finite elements for three-dimensional computations in electromagnetism", IEE Proc. Vol. **135**, A, No 8, 493-500 (1988).
 - [14] J. R. Shewchuk, Triangle - A Two-Dimensional Quality Mesh Generator and Delanunay Triangulator (version 1.5), June 4, 2004.
 - [15] C. V. Westenholz, *Differential Forms in Mathematical Physics*, Elsevier Science, North-Holland (1980).
 - [16] D. N. Arnold, Plenary address delivered at ICM (International Congress of Mathematicians), (2002).
 - [17] D. R. Tanner and A. F. Peterson, "Vector expansion functions for the numerical solution of Maxwell's equations," *Microwave and Opt. Tech. Lett.***14**, 331 (1989).
 - [18] J. M. Jin, *The Finite Element Method in Electromagnetics*, Wiley, New York, (2002).
 - [19] For high order 1-forms [4], the *DoFs* of 1-forms could associate with the faces and volumes, but *do not* associate with the nodes.

APPENDIX A: STIFFNESS MATRIX: GEOMETRIC VIEWPOINT

Using 3D tetrahedral and cubic elements, respectively, we will show that stiffness matrix $[S]$ equals the multiplication of incidences and Hodge matrices

$$[S] = [d_{curl}^*] [\star_{\mu-1}] [d_{curl}] \quad (\text{A1})$$

1. Tetrahedral elements

From the *DoFs* for the tetrahedral element (Fig. 3)

$$\mathbb{B} = \left[b_{1,2,3} \ b_{1,3,4} \ b_{1,4,2} \ b_{2,4,3} \right]^t \quad (\text{A2})$$

$$\mathbb{E} = \left[e_{1,2} \ e_{1,3} \ e_{1,4} \ e_{2,3} \ e_{4,2} \ e_{3,4} \right]^t \quad (\text{A3})$$

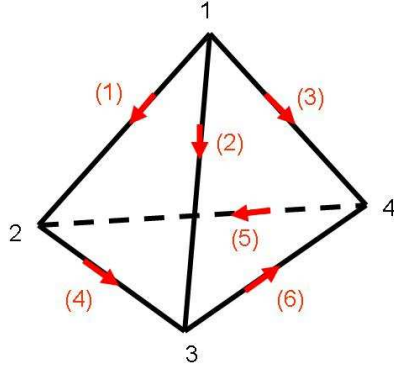


FIG. 3: Tetrahedral element.

we can construct the incidence matrices $[d_{curl}]$ and $[d_{curl}^*]$

$$[d_{curl}] = \begin{bmatrix} 1 & -1 & 0 & 1 & 0 & 0 \\ 0 & 1 & -1 & 0 & 0 & 1 \\ -1 & 0 & 1 & 0 & 1 & 0 \\ 0 & 0 & 0 & -1 & -1 & -1 \end{bmatrix} \quad (\text{A4})$$

$$[d_{curl}^*] = \begin{bmatrix} 1 & 0 & -1 & 0 \\ -1 & 1 & 0 & 0 \\ 0 & -1 & 1 & 0 \\ 1 & 0 & 0 & -1 \\ 0 & 0 & 1 & -1 \\ 0 & 1 & 0 & -1 \end{bmatrix} \quad (\text{A5})$$

Using 3D Whitney 2-form, the Hodge matrix $[\star_{\mu^{-1}}]$ can be calculated by the vector calculus proxies of Galerkin's Hodges

$$[\star_{\mu^{-1}}]_{\{(i,j,k),(\tilde{i},\tilde{j},\tilde{k})\}} = \int \frac{1}{\mu} \vec{W}_{i,j,k}^2 \cdot \vec{W}_{\tilde{i},\tilde{j},\tilde{k}}^2 dV \quad (\text{A6})$$

Let $[G] = [d_{curl}^*] [\star_{\mu^{-1}}] [d_{curl}]$. The matrix $[G]$ can be computed as

$$\begin{aligned}
[G] &= [d_{curl}^*] [\star_{\mu^{-1}}] [d_{curl}] \\
&= \begin{bmatrix} 1 & 0 & -1 & 0 \\ -1 & 1 & 0 & 0 \\ 0 & -1 & 1 & 0 \\ 1 & 0 & 0 & -1 \\ 0 & 0 & 1 & -1 \\ 0 & 1 & 0 & -1 \end{bmatrix} \begin{bmatrix} [\star_{\mu^{-1}}]_{11} & [\star_{\mu^{-1}}]_{12} & [\star_{\mu^{-1}}]_{13} & [\star_{\mu^{-1}}]_{14} \\ [\star_{\mu^{-1}}]_{21} & [\star_{\mu^{-1}}]_{22} & [\star_{\mu^{-1}}]_{23} & [\star_{\mu^{-1}}]_{24} \\ [\star_{\mu^{-1}}]_{31} & [\star_{\mu^{-1}}]_{32} & [\star_{\mu^{-1}}]_{33} & [\star_{\mu^{-1}}]_{34} \\ [\star_{\mu^{-1}}]_{41} & [\star_{\mu^{-1}}]_{42} & [\star_{\mu^{-1}}]_{43} & [\star_{\mu^{-1}}]_{44} \end{bmatrix} \\
&\quad \begin{bmatrix} 1 & -1 & 0 & 1 & 0 & 0 \\ 0 & 1 & -1 & 0 & 0 & 1 \\ -1 & 0 & 1 & 0 & 1 & 0 \\ 0 & 0 & 0 & -1 & -1 & -1 \end{bmatrix} \tag{A7}
\end{aligned}$$

which is a 6×6 matrix. The entry of stiffness matrix $[S]$ can be computed as

$$\begin{aligned}
[S]_{\{(i,j),(\tilde{i},\tilde{j})\}} &= \int \frac{1}{\mu} (\vec{\nabla} \times \vec{W}_{i,j}^1) \cdot (\vec{\nabla} \times \vec{W}_{\tilde{i},\tilde{j}}^1) dV \\
&= \frac{1}{\mu} (2\vec{\nabla} \zeta_i \times \vec{\nabla} \zeta_j) \cdot (2\vec{\nabla} \zeta_{\tilde{i}} \times \vec{\nabla} \zeta_{\tilde{j}}) \tag{A8}
\end{aligned}$$

By comparing each term of matrix (A7) with the corresponding term of matrix (A8), such as $[G]_{12}$

$$[G]_{12} = -[\star_{\mu^{-1}}]_{11} + [\star_{\mu^{-1}}]_{31} + [\star_{\mu^{-1}}]_{12} - [\star_{\mu^{-1}}]_{32} \tag{A9}$$

$$= \frac{1}{\mu} (2\vec{\nabla} \zeta_1 \times \vec{\nabla} \zeta_2) \cdot (2\vec{\nabla} \zeta_{\tilde{1}} \times \vec{\nabla} \zeta_{\tilde{3}}) \tag{A10}$$

and $[S]_{12}$

$$[S]_{12} = \frac{1}{\mu} (2\vec{\nabla} \zeta_1 \times \vec{\nabla} \zeta_2) \cdot (2\vec{\nabla} \zeta_{\tilde{1}} \times \vec{\nabla} \zeta_{\tilde{3}}) \tag{A11}$$

we obtain

$$[S] = [d_{curl}^*] [\star_{\mu^{-1}}] [d_{curl}] \tag{A12}$$

$$\begin{aligned}
\vec{N}_{1,2}^1 &= \frac{1}{L^3} \left(y_c + \frac{L}{2} - y \right) \left(z_c + \frac{L}{2} - z \right) \hat{x} \\
\vec{N}_{4,3}^1 &= \frac{1}{L^3} \left(-y_c + \frac{L}{2} + y \right) \left(z_c + \frac{L}{2} - z \right) \hat{x} \\
\vec{N}_{5,6}^1 &= \frac{1}{L^3} \left(y_c + \frac{L}{2} - y \right) \left(-z_c + \frac{L}{2} + z \right) \hat{x} \\
\vec{N}_{8,7}^1 &= \frac{1}{L^3} \left(-y_c + \frac{L}{2} + y \right) \left(-z_c + \frac{L}{2} + z \right) \hat{x} \\
\vec{N}_{1,4}^1 &= \frac{1}{L^3} \left(z_c + \frac{L}{2} - z \right) \left(x_c + \frac{L}{2} - x \right) \hat{y} \\
\vec{N}_{5,8}^1 &= \frac{1}{L^3} \left(-z_c + \frac{L}{2} + z \right) \left(x_c + \frac{L}{2} - x \right) \hat{y} \\
\vec{N}_{2,3}^1 &= \frac{1}{L^3} \left(z_c + \frac{L}{2} - z \right) \left(-x_c + \frac{L}{2} + x \right) \hat{y} \\
\vec{N}_{6,7}^1 &= \frac{1}{L^3} \left(-z_c + \frac{L}{2} + z \right) \left(-x_c + \frac{L}{2} + x \right) \hat{y} \\
\vec{N}_{1,5}^1 &= \frac{1}{L^3} \left(x_c + \frac{L}{2} - x \right) \left(y_c + \frac{L}{2} - y \right) \hat{z} \\
\vec{N}_{2,6}^1 &= \frac{1}{L^3} \left(-x_c + \frac{L}{2} + x \right) \left(y_c + \frac{L}{2} - y \right) \hat{z} \\
\vec{N}_{4,8}^1 &= \frac{1}{L^3} \left(x_c + \frac{L}{2} - x \right) \left(-y_c + \frac{L}{2} + y \right) \hat{z} \\
\vec{N}_{3,7}^1 &= \frac{1}{L^3} \left(-x_c + \frac{L}{2} + x \right) \left(-y_c + \frac{L}{2} + y \right) \hat{z}
\end{aligned} \tag{A17}$$

The corresponding face elements $\vec{N}_{i,j,k,l}^2$ can be constructed as

$$\begin{aligned}
\vec{N}_{1,4,3,2}^2 &= -\frac{1}{L^3} \left(z_c + \frac{L}{2} - z \right) \hat{z} \\
\vec{N}_{5,6,7,8}^2 &= \frac{1}{L^3} \left(z - z_c + \frac{L}{2} \right) \hat{z} \\
\vec{N}_{2,3,7,6}^2 &= \frac{1}{L^3} \left(x - x_c + \frac{L}{2} \right) \hat{x} \\
\vec{N}_{1,5,8,4}^2 &= -\frac{1}{L^3} \left(x_c + \frac{L}{2} - x \right) \hat{x} \\
\vec{N}_{1,2,6,5}^2 &= -\frac{1}{L^3} \left(y_c + \frac{L}{2} - y \right) \hat{y} \\
\vec{N}_{3,4,8,7}^2 &= \frac{1}{L^3} \left(y - y_c + \frac{L}{2} \right) \hat{y}
\end{aligned} \tag{A18}$$

The Hodge matrix $[\star_{\mu^{-1}}]$ can be calculated by the vector calculus proxies of Galerkin's Hodges

$$[\star_{\mu^{-1}}]_{\{(i,j,k,l),(\tilde{i},\tilde{j},\tilde{k},\tilde{l})\}} = \int \frac{1}{\mu} \vec{W}_{i,j,k,l}^2 \cdot \vec{W}_{\tilde{i},\tilde{j},\tilde{k},\tilde{l}}^2 dV \quad (\text{A19})$$

$$[\star_{\mu^{-1}}] = \frac{1}{6L\mu} \begin{bmatrix} 2 & -1 & 0 & 0 & 0 & 0 \\ -1 & 2 & 0 & 0 & 0 & 0 \\ 0 & 0 & 2 & -1 & 0 & 0 \\ 0 & 0 & -1 & 2 & 0 & 0 \\ 0 & 0 & 0 & 0 & 2 & -1 \\ 0 & 0 & 0 & 0 & -1 & 2 \end{bmatrix} \quad (\text{A20})$$

Let $c = \frac{1}{6L\mu}$. The matrix $[G]$ can be computed as

$$[G] = [d_{curl}^*] [\star_{\mu^{-1}}] [d_{curl}]$$

$$= c \begin{bmatrix} 4 & -1 & -1 & -2 & -2 & -1 & 2 & 1 & -2 & 2 & -1 & 1 \\ -1 & 4 & -2 & -1 & 2 & 1 & -2 & -1 & -1 & 1 & -2 & 2 \\ -1 & -2 & 4 & -1 & -1 & -2 & 1 & 2 & 2 & -2 & 1 & -1 \\ -2 & -1 & -1 & 4 & 1 & 2 & -1 & -2 & 1 & -1 & 2 & -2 \\ -2 & 2 & -1 & 1 & 4 & -1 & -1 & -2 & -2 & -1 & 2 & 1 \\ -1 & 1 & -2 & 2 & -1 & 4 & -2 & -1 & 2 & 1 & -2 & -1 \\ 2 & -2 & 1 & -1 & -1 & -2 & 4 & -1 & -1 & -2 & 1 & 2 \\ 1 & -1 & 2 & -2 & -2 & -1 & -1 & 4 & 1 & 2 & -1 & -2 \\ -2 & -1 & 2 & 1 & -2 & 2 & -1 & 1 & 4 & -1 & -1 & -2 \\ 2 & 1 & -2 & -1 & -1 & 1 & -2 & 2 & -1 & 4 & -2 & -1 \\ -1 & -2 & 1 & 2 & 2 & -2 & 1 & -1 & -1 & -2 & 4 & -1 \\ 1 & 2 & -1 & -2 & 1 & -1 & 2 & -2 & -2 & -1 & -1 & 4 \end{bmatrix} \quad (\text{A21})$$

Using the formula

$$[S]_{\{(i,j),(\tilde{i},\tilde{j})\}} = \int \frac{1}{\mu} \left(\vec{\nabla} \times \vec{N}_{i,j}^1 \right) \cdot \left(\vec{\nabla} \times \vec{N}_{\tilde{i},\tilde{j}}^1 \right) dV \quad (\text{A22})$$

the stiffness matrix $[S]$ can be computed as

$$[S] = c \begin{bmatrix} 4 & -1 & -1 & -2 & -2 & -1 & 2 & 1 & -2 & 2 & -1 & 1 \\ -1 & 4 & -2 & -1 & 2 & 1 & -2 & -1 & -1 & 1 & -2 & 2 \\ -1 & -2 & 4 & -1 & -1 & -2 & 1 & 2 & 2 & -2 & 1 & -1 \\ -2 & -1 & -1 & 4 & 1 & 2 & -1 & -2 & 1 & -1 & 2 & -2 \\ -2 & 2 & -1 & 1 & 4 & -1 & -1 & -2 & -2 & -1 & 2 & 1 \\ -1 & 1 & -2 & 2 & -1 & 4 & -2 & -1 & 2 & 1 & -2 & -1 \\ 2 & -2 & 1 & -1 & -1 & -2 & 4 & -1 & -1 & -2 & 1 & 2 \\ 1 & -1 & 2 & -2 & -2 & -1 & -1 & 4 & 1 & 2 & -1 & -2 \\ -2 & -1 & 2 & 1 & -2 & 2 & -1 & 1 & 4 & -1 & -1 & -2 \\ 2 & 1 & -2 & -1 & -1 & 1 & -2 & 2 & -1 & 4 & -2 & -1 \\ -1 & -2 & 1 & 2 & 2 & -2 & 1 & -1 & -1 & -2 & 4 & -1 \\ 1 & 2 & -1 & -2 & 1 & -1 & 2 & -2 & -2 & -1 & -1 & 4 \end{bmatrix} \quad (\text{A23})$$

Comparison of Eq.(A21) and Eq.(A23) gives the following identity

$$[S] = [d_{curl}^*] [\star_{\mu-1}] [d_{curl}] \quad (\text{A24})$$

The above proof can be straightforwardly extended to the rectangular brick element whose side lengths are (L_x, L_y, L_z) .